

Finite volume study of electric polarizabilities from lattice QCD.

Michael Lujan*, Andrei Alexandru, Walter Freeman, and Frank Lee

The George Washington University, Washington DC, USA

E-mail:

mlujan@gwmail.gwu.edu, aalexan@gwu.edu, wfreeman@gwu.edu, fxlee@gwu.edu

Knowledge of the electric polarizability is crucial to understanding the interactions of hadrons with electromagnetic fields. The neutron polarizability is very sensitive to the quark mass and is expected to diverge in the chiral limit. Here we present results for the electric polarizability of the neutron, neutral pion, and neutral kaon on eight ensembles with nHYP-smearred clover dynamical fermions with two different pion masses (227 and 306 MeV). These are currently the lightest pion masses used in polarizability studies. For each pion mass we compute the polarizability at four different volumes and perform an infinite volume extrapolation for the three hadrons. Along with the infinite volume extrapolation we conduct a chiral extrapolation for the kaon polarizability to the physical point. We compare our results for the neutron polarizability to predictions from chiral perturbation theory.

*32nd International Symposium on Lattice Field Theory - LATTICE 2014
June 23 - June 28, 2014
New York, USA*

*Speaker.

1. Introduction

To lowest order, the response of a composite particle to an electromagnetic field can be parameterized by the effective Hamiltonian:

$$\mathcal{H}_{em} = -\vec{p} \cdot \vec{\mathcal{E}} - \vec{\mu} \cdot \vec{B} - \frac{1}{2} (\alpha \mathcal{E}^2 + \beta B^2) + \dots, \quad (1.1)$$

where \vec{p} and $\vec{\mu}$ are the electric and magnetic dipole moments, respectively, and α and β are the electric and magnetic polarizabilities. Due to time-reversal symmetry of the strong interaction the electric dipole moment vanishes. Furthermore, by considering the simplified case of a weak constant electric field, the leading order interaction comes from the polarizability term at $\mathcal{O}(\mathcal{E}^2)$. The polarizability is a first-order structure constant which measures the rigidity of the hadron in the presence of the external field.

In this work, we use lattice QCD to compute the electric polarizability (α). We employ the background field method to extract the polarizability. Previous lattice calculations [1, 2, 3, 4, 5, 6] were done at relatively heavy pion masses leaving the chiral region largely unexplored. Here, we use 2-flavor n-HYP clover fermions with two different pion masses (227 MeV and 306 MeV) to study the chiral behavior of the polarizability. Moreover, for each mass we compute α on four different lattice volumes to study the volume dependence.

We analyze three neutral hadrons: neutral pion, neutral kaon, and the neutron. For each hadron we performed an infinite volume extrapolation. For the kaon, we also performed a chiral extrapolation to the physical point. The results of our neutron polarizability, will be compared to predictions from chiral perturbation theory. We note that our work, though done on dynamical configurations, uses electrically-neutral sea quarks throughout.

The outline of the paper is as follows: In section 2 we discuss the lattice methodology to extract the polarizability and our fitting procedure. In section 3 we present our results for the neutron, neutral pion and neutral kaon polarizability. We then summarize and present an outlook in section 4.

2. Methodology

2.1 Background field method

We use the background field method to place the electric field on the lattice. The method uses minimal coupling which augments the static electromagnetic vector potential (A_μ) to the covariant derivative, i.e.

$$D_\mu = \partial_\mu - igG_\mu - iqA_\mu, \quad (2.1)$$

where G_μ are the gluon field degrees of freedom. In practice, this amounts to an overall multiplicative phase factor to the original gauge links which appear in D_μ :

$$U_\mu \rightarrow e^{-iqaA_\mu} U_\mu. \quad (2.2)$$

The polarizability is extracted by computing the variation of the hadron's ground state energy with and without the presence of an electric field.

In order to extract the polarizability we need to use a weak enough electric field so that higher order terms in the field expansion can be safely neglected. In this work we instead use Dirichlet boundary conditions (DBC). The advantage of this is that we can use arbitrarily small values of the field. DBC also protects against the vacuum instability due to the Schwinger mechanism [7].¹ However, using DBC creates boundary effects. One of them is the introduction of a non-zero momentum for the hadron of magnitude π/L . The lowest energy state of the system is then $E = \sqrt{m^2 + (\pi/L)^2}$, where m is the mass of the hadron. To account for this motion we compute the mass shift (δm) motion due to the polarizability using the relation

$$\delta m = \delta E \frac{E}{m}. \quad (2.3)$$

The hadron's mass (m) is computed using periodic boundary conditions.

2.2 Fitting Procedure

The form of the correlators, for neutral hadrons in an constant electric field, retain their exponential fall off, allowing us to use some of the standard spectroscopy techniques to measure the shift in hadrons' energies.

The main difference in the fitting analysis is the fact that we need to extract the energy shift from the three correlation functions: $G_0, G_{+\eta}$, and $G_{-\eta}$, which are the correlation functions for the zero-field, and non-zero fields in the positive and negative x -direction, respectively. Since all three correlators are computed from the set of gauge configurations they are highly correlated; we therefore need to properly account for the correlations among them. To do this we construct the following difference vector as

$$\begin{aligned} \mathbf{v}_i &\equiv f(t_i) - \langle G_0(t_i) \rangle, \\ \mathbf{v}_{N+i} &\equiv \tilde{f}(t_i) - \langle G_{+\mathcal{E}}(t_i) \rangle, \\ \mathbf{v}_{2N+i} &\equiv \tilde{f}(t_i) - \langle G_{-\mathcal{E}}(t_i) \rangle \quad \text{for } i = 1, \dots, N \end{aligned} \quad (2.4)$$

where $t_1 \dots t_N$ is the fit window, $f(t) = A e^{-Et}$ and $\tilde{f}(t) = (A + \delta A) e^{-(E + \delta E)t}$. We minimize the χ^2 function,

$$\chi^2 = \mathbf{v}^\dagger \mathbf{C}^{-1} \mathbf{v},$$

in the usual fashion, where \mathbf{C} is the $3N \times 3N$ correlation matrix which encodes the correlations among the three different correlators.

3. Ensemble Details and Results

In this work we use 2-flavor nHYP-clover fermions [8] with two different pion masses (227 MeV and 306 MeV) in order to study the chiral behavior of the polarizability. For each pion mass we compute α on four different volumes in order to study the volume effects of the polarizability.

¹This instability only occurs for real electric fields and not for imaginary electric fields as used in most lattice studies. However, to use imaginary fields we need to rely on the analyticity of the theory around the point where the electric field is zero. Schwinger mechanism signals that this is not an analytical point generically. DBC offers one way to restore this analyticity.

Ensemble	Lattice	a (fm)	κ	N_c
EN1	$16 \times 16^2 \times 32$	0.1245	0.12820	230
EN2	$24 \times 24^2 \times 48$	0.1245	0.12820	300
EN3	$30 \times 24^2 \times 48$	0.1245	0.12820	300
EN4	$48 \times 24^2 \times 48$	0.1245	0.12820	270
EN5	$16 \times 16^2 \times 32$	0.1215	0.12838	230
EN6	$24 \times 24^2 \times 64$	0.1215	0.12838	450
EN7	$28 \times 24^2 \times 64$	0.1215	0.12838	670
EN8	$32 \times 24^2 \times 64$	0.1215	0.12838	500

Table 1: Details of the lattice ensembles used in this work. N_c is the number of configurations. The separation between the top four ensembles and bottom four ensembles is used to indicate the two different sea quark masses more clearly.

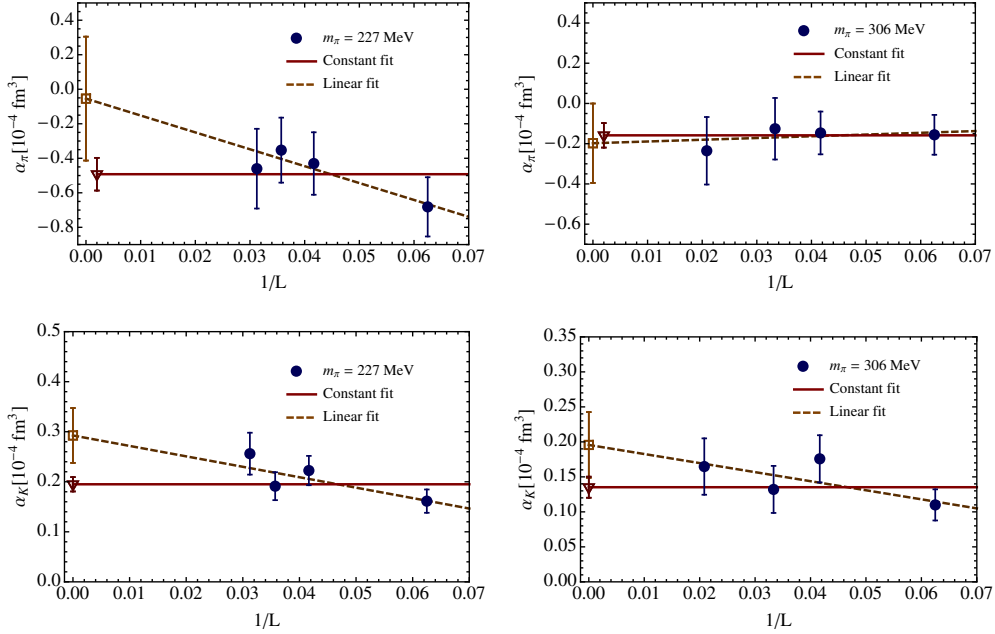


Figure 1: Top: Neutral pion polarizability as a function of $1/L$. The right panel are our results for the 306 MeV ensemble and the left panel corresponds to the 227 MeV ensemble. On each plot we overlay our infinite volume extrapolations using a constant (red-solid line) and linear (orange-dash line) fit. Bottom: Same as top graphs but for the neutral kaon.

A description of the ensembles are tabulated in Table 1. In our simulations we use a field size of $\eta \equiv a^2 q_d \mathcal{E} = 10^{-4}$, where q_d is the charge of the down quark. For a detailed discussion for the choice of η we refer the reader to our previous work [9].

3.1 Finite Volume Effects

The polarizabilities for the neutral pion, neutral kaon, and neutron were extracted for each

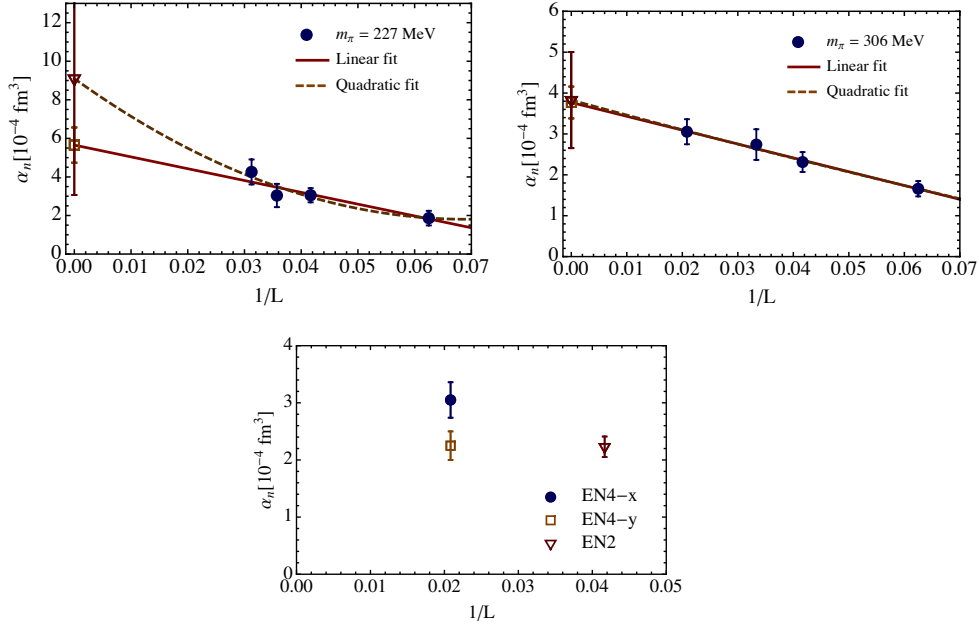


Figure 2: Top: Infinite volume extrapolation for the neutron polarizability. Bottom: Comparison of the EN2 ensemble to the results of the EN4 ensemble with the electric field in the x direction and with the electric field in the y direction. See text for details.

ensemble using the fitting procedure described in Sec. 2.2. For a given pion mass we studied the infinite volume behavior of the polarizability by extrapolating to the infinite volume limit using various polynomial degrees as fit models. We found, for the pion, that a constant extrapolation describes the data well. For the neutron and kaon we used a linear approximation. Figures 1 and 2 illustrate the results of the infinite volume extrapolation for both pion masses.

The volume dependence analysis assumes that the finite size corrections are mainly driven by the extent of the lattice in the direction of the electric field (which is in x -direction for this work). To verify this, we take our EN4 lattice which has the spatial dimension 48×24^2 and place the electric field along the y -direction which has only 24 lattice units. We choose this ensemble because the difference in the x and y directions are the largest which gives us the best comparison. If the finite volume corrections associated with the transverse directions are small, we expect our results to be comparable to the results of the EN2 ensemble which has the spatial dimension 24×24^2 . We display our results on the bottom panel of Fig. 2 for the EN2 lattice and the EN4 lattice for the electric field in the x direction and the electric field in the y direction. Our expectations are in very good agreement with our findings. That is, we found that dominant source of the finite size effects are connected to the extent of the lattice in the direction of the field.

3.2 Chiral Behavior

In this section we analyze the pion mass behavior for each of the particles we analyzed. On the left panel of Fig. 3 we plot our infinite volume extrapolation results for the pion polarizability as a function of m_π . We also include the values calculated by Detmold *et al.* [3] at $m_\pi = 390 \text{ MeV}$

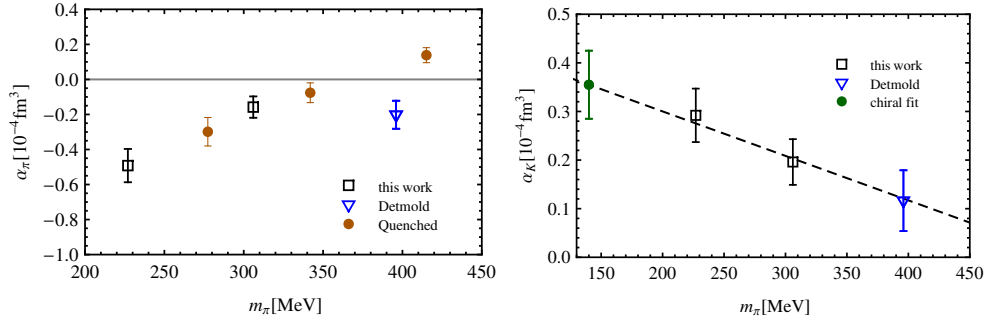


Figure 3: Left panel: Pion mass dependence of the pion polarizability. The orange/circle points are quenched results found in [10] and the blue/triangle point is the value determined in [3]. Right panel: Pion mass dependence for the kaon polarizability along with a chiral fit which includes the value determined in [3]

along with quenched results calculated by Alexandru and Lee [10]. The negative trend, which has been seen in our previous work [11], is still present; determining its origin is an ongoing study.

Our results for the kaon polarizability is illustrated on the right panel of Fig. 3. The plot also includes the value determined by Detmold *et al.* [3]. The kaon polarizability becomes larger as we lower the pion mass. In our previous work [9] we performed an extrapolation to the physical point using only the EN2 and EN6 lattices. We had found $\alpha_K = 0.269(43) \times 10^{-4} \text{ fm}^3$. Here we do the same analysis but now using our infinite volume results together with the value determined in [3]. We find $\alpha_K = 0.355(70) \times 10^{-4} \text{ fm}^3$. In this fit we assumed that the finite volume corrections at $m_\pi = 390 \text{ MeV}$ are small since they seem to decrease as we increase the pion mass.

On the left panel of Fig. 4 we plot our infinite volume results for the neutron polarizability as a function of m_π along with quenched data that were computed in [10]. We also compare our data to two different χ PT predictions: χ PT1 [12, 13] and χ PT2 [14] to gauge systematic errors of our calculation. For a more detailed comparison of the two χ PT predictions we refer the reader to [9].

Similar to our findings in [9], which only analyzed the EN2 and EN6 ensembles, we find that our infinite volume results are compatible with the quenched ones. Moreover, our results are now in excellent agreement with the χ PT1 curve. This was not the case for our previous analysis which did not take into account the volume effects. In Fig. 4 we add the experimental point along with two other lattice calculations [2, 1] for the neutron polarizability. Our results have the smallest pion masses used in polarizability studies and the smallest statistical errors.

4. Conclusion

We have presented a calculation of the electric polarizabilities for the neutron, neutral pion, and neutral kaon in the framework of lattice QCD. We used two different pion masses (227 MeV and 306 MeV) to study the chiral behavior of the polarizability. Currently, these are the smallest masses used in polarizability studies. We employed the background field method along with Dirichlet boundary conditions to place a constant electric field onto the lattice. A finite volume study was performed for each pion mass by computing the polarizability on four different lattice volumes. This was one of the most important results in this work. For the neutron we find that the finite

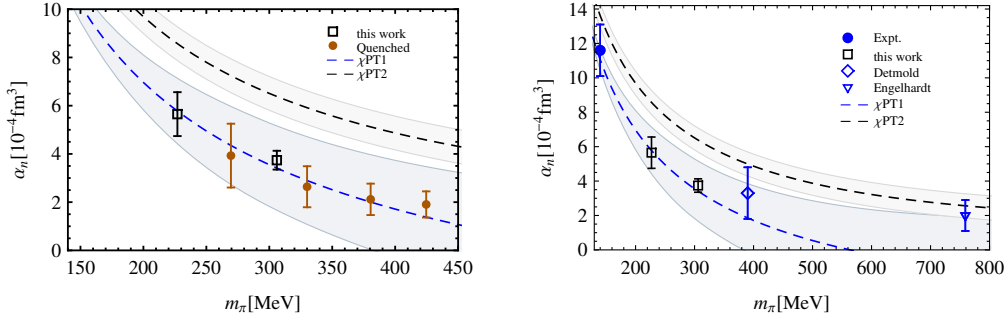


Figure 4: Left panel: Pion mass dependence of the neutron polarizability. The orange/circle points are quenched results found in [10]. The dashed lines are two different curves predicted by χ PT1 [12, 13] and χ PT2 [14]. Right panel: Plot of our results along with the experimental value and two other lattice calculations [1] and [2].

volume corrections are significant. Without the infinite volume extrapolation our results did not agree with χ PT calculations at our lowest pion mass where χ PT is expected to be more accurate.

5. Acknowledgements

This work was done on the following GPU clusters: GWU IMPACT clusters, GWU CCAS Colonial One cluster, JLab clusters, Fermilab clusters, and UK clusters. This work is supported in part by the NSF CAREER grant PHY-1151648 and the U.S. Department of Energy grant DE-FG02-95ER-40907.

References

- [1] M. Engelhardt (LHPC Collaboration), *Phys.Rev.* **D76** (2007) 114502, [[arXiv:0706.3919](#)].
- [2] W. Detmold, B. Tiburzi, and A. Walker-Loud, *Phys.Rev.* **D81** (2010) 054502, [[arXiv:1001.1131](#)].
- [3] W. Detmold, B. C. Tiburzi, and A. Walker-Loud, *Phys.Rev.* **D79** (2009) 094505, [[arXiv:0904.1586](#)].
- [4] H. Fiebig, W. Wilcox, and R. Woloshyn, *Nucl.Phys.* **B324** (1989) 47.
- [5] A. Alexandru and F. X. Lee, *PoS LAT2009* (2009) 144, [[arXiv:0911.2520](#)].
- [6] A. Alexandru and F. X. Lee, *PoS LATTICE2008* (2008) 145, [[arXiv:0810.2833](#)].
- [7] J. S. Schwinger, *Phys.Rev.* **82** (1951) 664–679.
- [8] A. Hasenfratz, R. Hoffmann, and S. Schaefer, *JHEP* **0705** (2007) 029, [[hep-lat/0702028](#)].
- [9] M. Lujan, A. Alexandru, W. Freeman, and F. Lee, [[arXiv:1310.4837](#)].
- [10] A. Alexandru and F. Lee, *PoS LATTICE2010* (2010) 131, [[arXiv:1011.6309](#)].
- [11] M. Lujan, A. Alexandru, and F. Lee, *PoS LATTICE2011* (2011) 165, [[arXiv:1111.6288](#)].
- [12] H. Griesshammer, J. McGovern, D. Phillips, and G. Feldman, *Prog.Part.Nucl.Phys.* **67** (2012) 841–897, [[arXiv:1203.6834](#)].
- [13] J. McGovern, D. Phillips, and H. Griesshammer, *Eur.Phys.J.* **A49** (2013) 12, [[arXiv:1210.4104](#)].
- [14] V. Lensky and V. Pascalutsa, *Eur.Phys.J.* **C65** (2010) 195–209, [[arXiv:0907.0451](#)].